International Journal of Antimicrobial Agents 53 (2019) 362–369

Contents lists available at ScienceDirect

International Journal of Antimicrobial Agents

journal homepage: www.elsevier.com/locate/ijantimicag

# Spiramycin and azithromycin, safe for administration to children, exert antiviral activity against enterovirus A71 in vitro and in vivo

Shinuan Zeng[a,b], Xiaobin Meng[c], Qingyuan Huang[c], Nanfeng Lei[c], Lingbin Zeng[c], Xinying Jiang[b], Xuemin Guo[a,b,c,*]

[a] Institute of Human Virology, Zhongshan School of Medicine, Sun Yat-Sen University, Guangzhou 510080, China
[b] Key Laboratory of Tropical Disease Control (Sun Yat-Sen University), Ministry of Education, Guangzhou 510080, China
[c] Meizhou People's Hospital, Meizhou 514031, China

ARTICLE INFO

*Article history:*
Received 24 April 2018
Accepted 22 December 2018

*Keywords:*
Macrolide antibiotics
Enterovirus A71
Antiviral activity

ABSTRACT

Hand-foot-mouth disease (HFMD) is a common viral disease in young children, mainly caused by enterovirus A71 (EV-A71) and coxsackievirus A16 (CV-A16). Specific antiviral agents are not commercially available yet. Here we report that the macrolide antibiotics spiramycin (SPM) and azithromycin (AZM) possess antiviral activities against EV-A71 and CV-A16. SPM significantly reduced EV-A71 RNA and protein levels, most likely through interfering with viral RNA replication. The SPM-resistant EV-A71 variants showed similar resistance to AZM, indicating a similar anti-EV-A71 mechanism by which these two drugs exert their functions. The mutations of these variants were reproducibly mapped to VP1 and 2A, which were confirmed to confer resistance to SPM. Animal experiments showed that AZM possesses stronger anti-infection efficacy than SPM, greatly alleviated the disease symptoms and increased the survival rate in a mouse model severely infected with EV-A71. In all, our work suggests that AZM is a potential treatment option for EV-A71-induced HFMD, whose proved safety for infants and children makes it even more promising.



## 1. Introduction

Hand-foot-mouth disease (HFMD) mainly occurs in children under 5 years of age and occasionally leads to severe neurological diseases and even death [1]. Enterovirus A71 (EV-A71) and coxsackievirus A16 (CV-A16) are recognized as the prominent causative agents [2]. Currently, there is no approved antiviral drug available for treatment of HFMD.

EV-A71 and CV-A16 are non-enveloped, single-stranded and positive-sense RNA viruses belonging to *Picornaviridae* family [3]. Their genome consists of a 5′ untranslated region (5′UTR) capped with a viral protein VPg, a single open reading frame (ORF) encoding a polyprotein and a poly(A)-tailed 3′UTR [4]. The 5′UTR harbors an internal ribosome entry site (IRES) that allows viral RNA translation [5]. The produced polyprotein is proteolytically processed by the viral proteases 2A and 3C into four structural proteins (VP1–VP4) and seven non-structural proteins (2A–2C and 3A–3D) [4]. EV-A71 has been extensively used as a target for HFMD drug development. A wide range of compounds have been reported to possess significant in vitro and/or in vivo activity against EV-A71 infection through variable action mechanisms during the past decades, including but not limited to EV-A71 structural or non-structural protein inhibitors, nucleotide analogs, type I interferon subtypes and antiviral peptides [6]. However, to our knowledge, few of them have reached the clinical trial stage. In vivo effectiveness and safety concerns are responsible for this huge gap between bench and bedside. Effective therapeutic drugs that can be used safely in children suffering from HFMD and serious complications are urgently needed.

Macrolide antibiotics are broad-spectrum bacteriostatic agents. They selectively bind to the bacterial 50S ribosomal subunit and subsequently repress translation [7]. Beyond antibacterial activity, macrolides also possess anti-inflammatory and immunomodulatory activities [8,9], which have led to their use in clinical treatment for diffuse panbronchiolitis (DPB) [10] and bronchiectasis [11]. Interestingly, macrolides have shown activity against the viruses causing respiratory infections, including respiratory syncytial virus, rhinovirus and influenza virus [12]. These antibiotics have been clinically proven to be safe in pregnant women, newborns and young children and are recommended as the first-line therapy for some infections [13,14]. Given all these features, it is worth examining whether macrolide antibiotics have activity

* Corresponding author. Zhongshan School of Medicine, Sun Yat-Sen University, Guangzhou 510080, China. Fax: +86 20 8733 2588.
*E-mail address:* xmguo2005@yahoo.com (X. Guo).

https://doi.org/10.1016/j.ijantimicag.2018.12.009
0924-8579/

against EV-A71 and CV-A16 and can thus be used for HFMD treatment.

Here we report that the macrolide antibiotics spiramycin (SPM) and azithromycin (AZM) exhibit antiviral activity against EV-A71 and CV-A16 in cell culture. Their in vivo anti-EV-A71 infection efficacy was examined in a mouse model. The mechanism of macrolides against EV-A71 was investigated using SPM as a representative.

## 2. Materials and methods

### 2.1. Cells, viruses and antimicrobial agents

Vero, RD, 293A, and 293A-SCARB2 cells were grown in DMEM supplemented with 10% foetal bovine serum (FBS; Gibco). EV-A71-GFP, a modified EV-A71 strain carrying GFP, was produced by transfecting 293A-SCARB2 cells with pWSK-EV71-GFP together with pcDNA3.1-T7RNP [15]. EV-A71-MZ (GenBank accession number KY582572) and CV-A16-GZ (GenBank accession number MG182694) were isolated from Meizhou People's Hospital and Guangzhou Women and Children's Medical Center, respectively. Macrolide antibiotics and ribavirin (Meilun Bio, China) were dissolved in dimethyl sulphoxide (DMSO) and saline, respectively.

### 2.2. Flow cytometry-based antiviral activity assay

293A-SCARB2 cells were seeded into a 24-well plate and incubated for 18∼24 h, then infected with EV-A71-GFP at a multiplicity of infection (MOI) of 0.1 plaque-forming units (PFU)/cell for 1 h, followed by addition of macrolide antibiotics; each treatment was performed in triplicate. Cells were collected at 18 h post-infection and used for GFP production assay through flow cytometry (FCM; BD LSRFortessa). The infected cells treated with DMSO alone were used as a control.

### 2.3. Cytotoxicity assay

293A-SCARB2 or Vero cells were seeded on to a 96-well plate with $1.5 \times 10^4$ cells per well. After incubation for 24 h, the cells were treated with different concentrations of SPM or AZM for 48 h. Cell viability was measured using CellTiter-Glo® Luminescent Cell Viability Assay Kit (Promega) according to the manufacturer's instructions. The cells treated with DMSO alone were used as a control. The cytotoxicity of macrolides was estimated by comparing the signal of the drug-treated cells with that of control cells.

### 2.4. Plaque reduction assay

Vero cells were seeded on to a six-well plate with $6 \times 10^5$ cells per well. After incubation for 24 h, the cells were infected with EV-A71-MZ or CV-A16-GZ (MOI, 0.1) and then treated with serially diluted SPM or AZM. After incubation for 36 h, the culture supernatants were collected and subjected to viral titre quantification by plaque assay. The 50% inhibitory concentration ($IC_{50}$), defined as SPM or AZM concentration required to achieve 50% of the maximal viral titre reduction, was calculated using GraphPad Prism 5 (GraphPad Software Inc., La Jolla, CA, USA).

### 2.5. Plaque assay

The plaque assay was performed as described previously [16], with RD cells replaced with Vero cells.

### 2.6. Time-of- addition assay

Vero cells were seeded on to a 12-well plate. After incubation for 24 h, the cells were infected with EV-A71-MZ (MOI, 5) for 1 h at 37°C followed by three times washing with phosphate-buffered saline (PBS). SPM was added to the cells 2 h before infection or at various times after infection. The culture supernatants were collected at 10 h after infection and titrated by plaque assay.

### 2.7. Viral attachment and endocytosis assay

293A-SCARB2 cells were seeded on to a 24-well plate filled with a coverslip in each well. After incubation for 12 h, the cells were infected with EV-A71-MZ (MOI, 100) for 1 h at 4°C to allow viral attachment. After washing three times with ice-cold PBS, the cells were fixed in 250 µl ice-cold 4% paraformaldehyde for 20 min and then permeabilized by 250 µl PBS containing 0.2% TritonX-100 for 10 min. Subsequently, the cells were washed with PBS containing 0.1% TritonX-100 three times and then blocked with 5.5% FBS in PBST (PBS with 0.1% Tween-20) for 30 min. The attached EV-A71 virions were detected with the anti-VP2 monoclonal antibody (Merck) followed by Alexa Fluor 555-conjugated donkey anti-mouse IgG (ThermoFisher). Nuclei were stained with DAPI (Life Technologies). The prepared samples were detected with a confocal microscope (Zeiss, LSM780). For endocytosis assay, the same performance was carried out, except that the cells were transferred to 37°C for additional 30-min incubation after incubation at 4°C to allow virus entry.

### 2.8. RNA isolation and reverse transcription-quantitative polymerase chain reaction

Vero cells were infected with EV-A71-MZ (MOI, 1). At different times post-infection, total RNA was isolated using TRIzol reagent (Invitrogen) following the manufacturer's instructions. Reverse transcription-quantitative polymerase chain reaction (RT-qPCR) was performed as described previously [17] with some modifications. Briefly, RNA was treated with DNase I (Promega); cDNAs were synthesized using the PrimeScript RT reagent Kit (Takara, Dalian) and then subjected to real-time PCR using TransStart Green qPCR SuperMix (Transgene) in Bio-Rad CFX96 thermocycler. EV-A71 2C RNA levels were normalized to those of GAPDH. The primers used are listed in Supplementary Table S1.

### 2.9. Bicistronic reporter plasmid construction

psiCHECK2 (Promega) contains an upstream *renilla* luciferase gene (*Rluc*) and a downstream firefly luciferase gene (*Fluc*), linked by an HSV-TK promoter. psiCHECK2-M was generated from psiCHECK2 by deleting HSV-TK promoter using reverse PCR with a pair of back-to-back primers containing a *Not*I or a *Sal*I restriction site. EV-A71-5′UTR was amplified from pWSK-EV71-GFP by PCR. After digestion with *Not*I and *Sal*I, the PCR products were linked into the similarly digested psiCHECK2-M and resulted in psiCHECK2-M-EV71-5′UTR. The primers used are listed in Supplementary Table S1.

### 2.10. In vitro transcription and RNA transfection

EV-A71-GFP RNAs and the EV-A71-5′UTR-containing bicistronic reporter RNAs were transcribed from linearized pWSK-EV71-GFP and psi-CHECK2-M-EV71-5′UTR, respectively, using a RiboMAX Large Scale RNA Production System (Promega). 293A cells were seeded on to a 24-well plate 18 h prior to transfection. The RNA transcripts were individually mixed with the Lipofectamine 2000 reagent (Invitrogen) at a ratio of 1:1.5 (µg:µL) and 1 µg RNA was

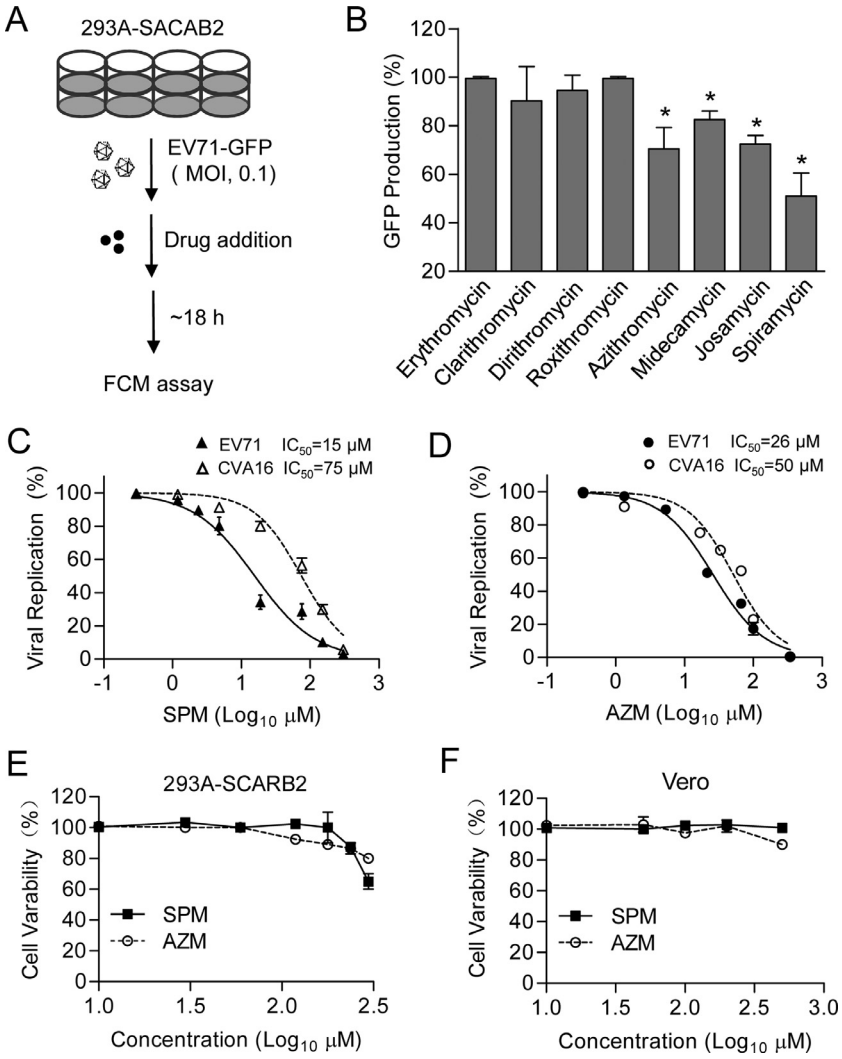


**Fig. 1.** Antiviral analyses of macrolide antibiotics against EV-A71 and CV-A16. (A) Schematic representation of a flow cytometry (FCM)-based antiviral activity assay. (B) Eight macrolide antibiotics were tested for the potential anti-EV-A71 activity. For each macrolide, 10 μM was used. GFP production is shown as a percentage of the fluorescence density from the mock-treated cells, i.e. dimethyl sulphoxide (DMSO)-treated cells, which was set as 100%. The antiviral activities of spiramycin (SPM) (C) and azithromycin (AZM) (D) against EV-A71-MZ and CV-A16-GZ were examined. Vero cells were infected with EV-A71-MZ or CV-A16-GZ (multiplicity of infection (MOI), 0.1), and then treated with two-fold serial dilutions of the drugs. The viral yields were determined by plaque assay, and the value from the cells treated with DMSO was set 100%. Viability of 293A-SCARB2 (E) and Vero cells (F) after treatment with different concentrations of SPM or AZM for 48 h were measured, with the value from the cells treated with DMSO set as 100%. The results are presented as mean ± standard deviation (SD) of three independent experiments. $^{*}P<0.05$. $IC_{50}$, 50% inhibitory concentration.

used for each well transfection. After incubation for 3 h at 37°C, the medium was replaced with fresh medium containing SPM or DMSO alone. GFP expression was observed at appropriate intervals by using a fluorescence microscope (Leica), and luciferase activity was measured.

### 2.11. Luciferase activity assay

Rluc and Fluc activities were measured as described previously [18].

### 2.12. Generation and sequencing of SPM-resistant EV-A71

Drug-resistant EV-A71 was selected as described previously [19] with some modifications. Briefly, EV-A71-MZ was passaged continuously in Vero cells in the presence of SPM at gradually increasing concentrations (Fig. 4A). Simultaneously, EV-A71-MZ was passaged continuously in the presence of DMSO alone as a negative control. Drug resistance was determined from the change in viral yield between EV-A71-MZ wild type (WT) and mutants in the presence of SPM. The selection was terminated when no further increase of resistance was observed. To identify the mutations responsible for SPM resistance, viral RNA was extracted from the selected virions with TRizol LS reagent (Invitrogen) and reverse-transcribed with PrimeScript RT reagent Kit (Takara, Dalian). PCRs were performed to recover the complete viral RNA genome as described previously [20]. The mutation sites were determined through PCR sequencing and subsequent sequence alignment with EV-A71-MZ WT.

### 2.13. Preparation of recombinant EV-A71-GFP variants

The EV-A71-GFP cDNA clones with different mutations were constructed based on pWSK-EV71-GFP, and the mutations were introduced by overlap extension PCR as described previously [21]. The primers used are listed in Supplementary Table S1. All the constructs were confirmed by DNA sequencing. After in vitro transcription, the full-length viral RNAs with different mutations were individually transfected into 293A-SCARB2 cells using Lipofectamine 2000 reagent to generate recombinant EV-A71-GFP

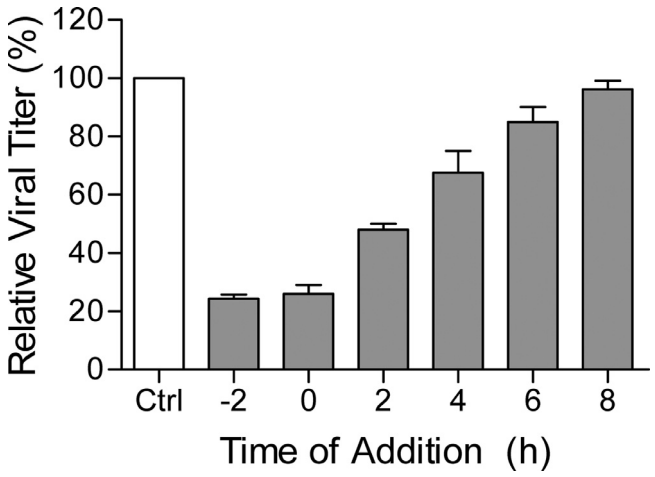


**Fig. 2.** Time-of-addition assay of spiramycin (SPM) inhibiting EV-A71 replication. Vero cells were infected with EV-A71 (multiplicity of infection (MOI), 5). The time of adding SPM (final concentration of 50 μM) was indicated. Ten hours post-infection, the viral yields were measured by plaque assay. The viral yield of the cells mock-treated with dimethyl sulphoxide (DMSO) was used as a control. The results are presented as mean ± standard deviation (SD) of three independent experiments.

variants. When CPE appeared, culture supernatants were collected, aliquoted and stored at −80°C for infection assay.

### 2.14. Preparation of mouse-adapted EV-A71 strain, mouse infection and drug treatment

BALB/c mice were purchased from the Laboratory Animal Center at Sun Yat-Sen University (Guangzhou, China). EV-A71-MZ was inoculated intraperitoneally (i.p.) into 1-day-old BALB/c mice. After multiplication for 5 days, the progeny virions were isolated from the limb tissues and again inoculated into 1-day-old BALB/c mice. After four passages in mice and one passage in RD cells, mouse-adapted EV-A71 strains were obtained. Five-day-old BALB/c mice were divided into five groups, with six mice in each group. Four out of the five groups were given the mouse-adapted EV-A71 i.p. at a dose of $10^7$ PFU per mouse, and then treated with SPM, AZM or ribavirin at a dose of 30 mg/kg once daily for five consecutive days or mock-treated with an equal volume of DMSO as a control. The remaining uninfected group was given saline as a healthy control. All the mice above were monitored daily for recording weight, clinical manifestations and death for 2 weeks post-infection.

### 2.15. Statistical analysis

The two-tailed Student's *t* test was used for statistical analysis by using GraphPad Prism 5. The survival curves in the murine infection model were analysed using the log-rank test in GraphPad Prism 5. Differences were considered statistically significant at $P<0.05$.

## 3. Results

### 3.1. SPM and AZM exhibit antiviral activities against EV-A71 and CV-A16 in vitro

For eight common macrolide antibiotics, the activity against EV71 multiplication was detected through an FCM-based assay (Fig. 1A). 293A-SCARB2 cells, which express the main EV-A71 receptor SCARB2, were used to facilitate the virus infection. Immediately after the EV-A71-GFP infection, the drugs, including erythromycin, clarithromycin, dirithromycin, roxithromycin, AZM, midecamycin, josamycin, and SPM, were individually added to the cells, reaching a final concentration of 10 μM. The GFP protein levels were correlated with viral yields. Of the eight macrolides, SPM showed significant inhibition on GFP production, followed by AZM, josamycin and midecamycin in order; while other tested macrolides only showed a weak inhibitory effect or no effect at all (Fig. 1B).

The antiviral activities of SPM and AZM were further evaluated against the clinical isolates of EV-A71 or CV-A16 through plaque reduction assay. Vero cells were infected with EV-A71-MZ or CV-A16-GZ followed by the addition of different concentrations of SPM or AZM. The viral yields were measured at 36 h post-infection. As shown in Fig. 1C and 1D, the $IC_{50}$ of SPM against EV-A71-MZ and CV-A16-GZ was 15 μM and 75 μM, respectively; those of AZM were 26 μM and 50 μM, respectively. Cytotoxicity assay revealed that the inhibition of viral replication was not related to macrolide-mediated cytotoxicity. Both SPM and AZM showed 15% cytotoxicity on 293A-SCARB2 cells at 178 μM (Fig. 1E) but no effect on Vero cell viability even at 250 μM (Fig. 1F). These results indicate that SPM and AZM exert anti-enterovirus activities, while their efficacies inhibiting EV-A71 are stronger than those inhibiting CV-A16. In addition, SPM inhibits EV-A71 replication more strongly than AZM in cell culture.

### 3.2. SPM represses the synthesis of viral RNA directly or indirectly

Due to the strong anti-EV-A71 activity of SPM, the mechanism behind the antiviral activity of SPM was investigated with time-of-addition assay. Vero cells were infected with EV-A71-MZ and then SPM was added at different times, followed by viral yield measurements at 10 h post-infection. Compared to the control cells, the viral yields reduced by approximately 77% in the cells treated with SPM at 2 h before infection and during infection (Fig. 2). When SPM was added at 2 h, 4 h and 6 h post-infection, the viral yields rebounded significantly and when SPM was added 8 h post-infection, the viral yield was back to the control level (Fig. 2). A full-round infection of EV-A71-MZ (MOI, 5) is about 8–10 h, which was estimated by monitoring the viral titre changes in the cell culture (Supplementary Fig. S1). These results indicate that SPM mainly inhibits EV-A71 replication at an early post-entry stage, however, a potential effect on viral assembly and release could not be excluded completely.

Whether SPM could affect EV-A71 attachment and endocytosis was further examined. As shown in Fig. 3A, EV71 virions attached equally to the surfaces of 293A-SARB2 cells in the absence or presence of SPM at 4°C. After transfer to 37°C and incubation for an additional 30 min, the attached viruses entered into the cells with no observed difference (Fig. 3A). These results confirmed that SPM does not interfere with EV-A71 attachment and endocytosis, consistent with the results of our time-of-addition assay (Fig. 2).

The effect of SPM on viral RNA production was detected by reverse transcription (RT)-PCR. SPM or DMSO was added to the medium immediately after EV-A71-MZ infection into Vero cells. RT-PCR assay showed that the viral RNA abundance in the SPM-treated cells was much lower than that in the mock-treated cells at each time point from 1 to 9 h post-infection (Fig. 3B), suggesting that SPM represses viral RNA synthesis directly or indirectly. To provide more evidence for this assumption, 293A cells were transfected with EV-A71-GFP genomic RNA, followed by SPM or DMSO treatment for 18 h. Compared to the control, the number of the GFP-positive cells reduced by 18% or 70% upon exposure to 10 μM or 50 μM of SPM, respectively (Fig. 3C). Given a crosslink between viral translation and RNA replication during the life cycle of EV-A71, these results indicate that SPM potentially inhibits EV-A71 replication by suppressing the synthesis of viral RNA, viral proteins, or both.

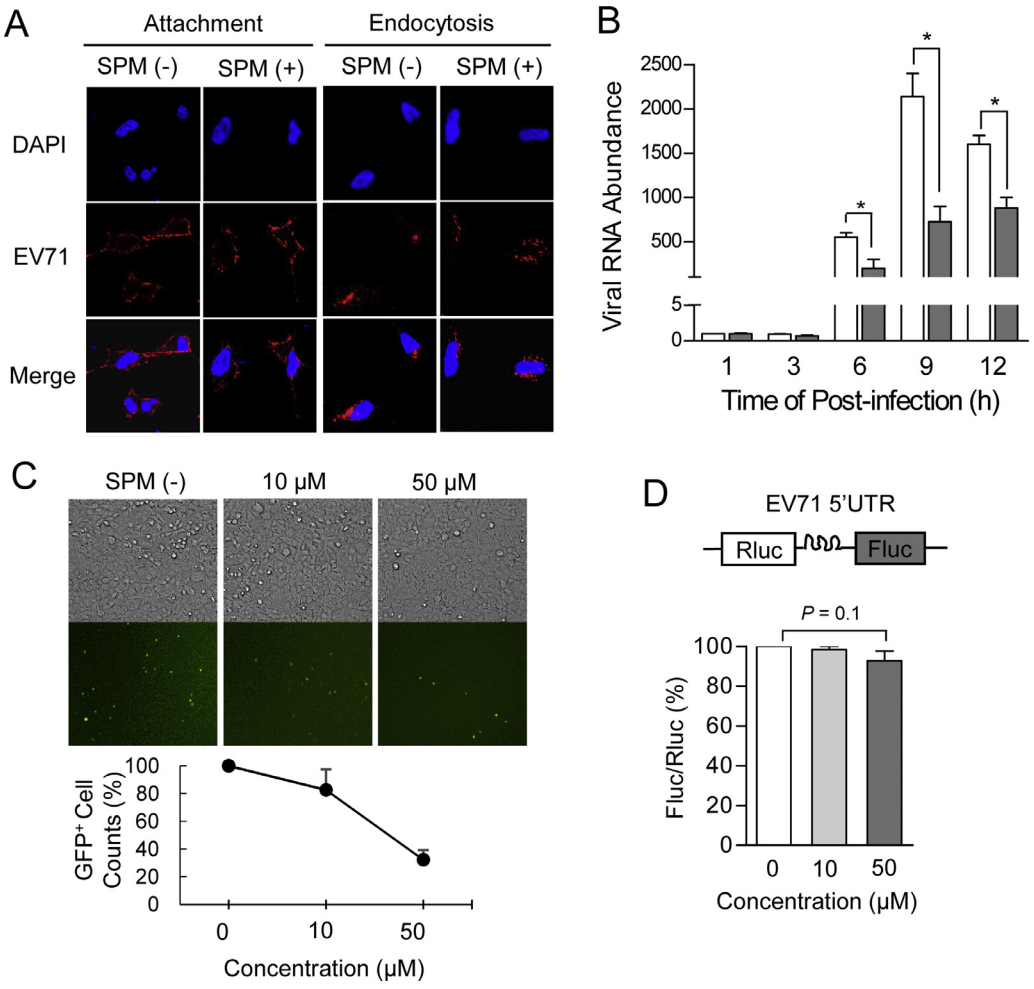


**Fig. 3.** Stage assays of spiramycin (SPM) against EV-A71. (A) Effect of SPM on the attachment and endocytosis of EV-A71. 293A-SCARB2 cells were infected with EV-A71-MZ (multiplicity of infection (MOI), 100) in the presence of SPM (50 μM) or dimethyl sulphoxide (DMSO; as a control). Virions were detected by immuno-fluorescence assay (IFA). (B) Reverse transcription-quantitative polymerase chain reaction (RT-qPCR) assay of viral RNA in the cells treated with SPM (50 μM) or mock-treated with DMSO. Total RNA was isolated at different times post-infection. The viral RNA level was normalized to that of *GAPDH* mRNAs, with the relative level at 1 h post-infection set as 1. (C) Effect of SPM on the protein production from the infectious viral RNAs. 293A cells were transfected with EV-A71-GFP RNA followed by addition of two different concentrations of SPM or DMSO. Expression of GFP was monitored at 18 h post-infection using a fluorescence microscope (upper panel). The GFP-positive ($GFP^+$) cells in 50 fields were counted and the relative mean number was calculated, with that of DMSO-treated cells set as 100% (lower panel). (D) Reporter assay of the effect of SPM on the EV-A71 internal ribosome entry site (IRES)-mediated translation. Diagram shows the bicistronic reporter system without or with EV-A71-5′UTR insertion (upper panel). The EV-A71-5′UTR-containing bicistronic reporter RNA was transfected into 293A cells, followed by treatment with different concentrations of SPM or DMSO. After incubation for 18 h, luciferase activity was measured (lower panel). Data are presented as mean ± standard deviation (SD) of three independent experiments.

The potential inhibition of EV-A71 translation by SPM was detected using a bicistronic reporter system, in which the Fluc translation is driven by EV-A71 IRES (Fig. 3D, upper panel). 293A cells were transfected with the reporter RNA containing EV-A71-5′UTR and then treated with SPM or DMSO alone. The reporter expression changed little in the SPM-treated cells compared with the mock-treated cells (Fig. 3D, lower panel), indicating that SPM has little effect on EV71 IRES-mediated translation. Altogether, these results indicate that SPM inhibits EV71 replication at post-entry stage, most likely through repressing viral RNA synthesis directly or indirectly.

### 3.3. Selection and determination of the mutations conferring resistance to SPM

SPM-resistant EV-A71 was selected and the mutations were determined to uncover the potential target(s) of SPM. The selection procedure is shown in Fig. 4A. Three independent selections were performed simultaneously and resulted in three surviving EV-A71-MZ pools, namely, SelA, SelB and SelC. Meanwhile, EV-A71-MZ was passaged successively for 18 rounds in the presence of DMSO alone, and the obtained virus pool was used as a control. Viral titre reduction assay was performed to examine whether the surviving viruses developed resistance to SPM as well as to AZM. As shown in Fig. 4B, all the viruses, whether the WT or the selected virus pools, showed very similar viral titres in the absence of the macrolides, indicating comparable virus replication efficiency. Upon exposure to 50 μM of SPM, the titres of the WT viruses reduced approximately 400-fold; in contrast, the titres of SelA, SelB and SelC reduced approximately 10-fold (Fig. 4B), showing a significant increase in the viral yields. Similar results were obtained when the viruses were exposed to 50 μM of AZM. These data indicate that SPM selection could make the viruses develop resistance to both SPM and AZM, revealing a similar action mechanism responsible for the anti-EV-A71 activity of these two macrolides.

The genomes of the control and the selected viruses were sequenced, and five sense mutations were identified, i.e. VP1-N102S, 2A-S7F, 2A-G8R, 2B-I47T and 2C-M108V (Fig. 4C). Noticeably, VP1-N102S was found in SelC and it was also the only mutation found in SelB, indicating an important role in conferring SPM resistance.

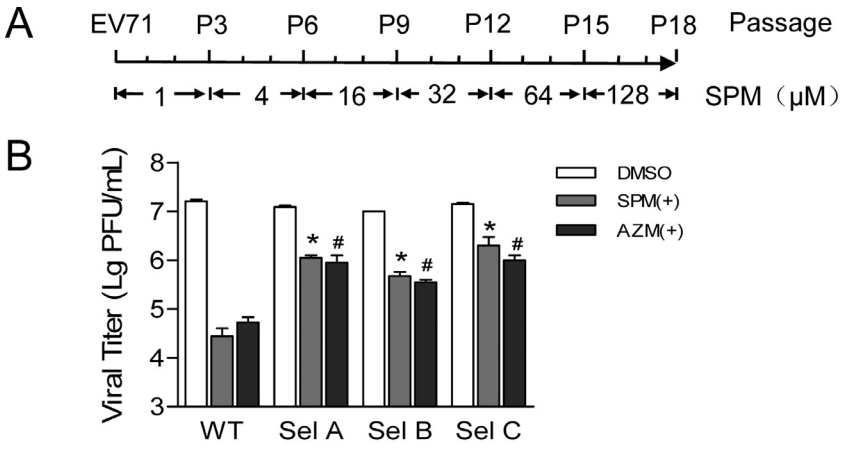


C

| | | VP1 | 2A | 2B | 2C |
|---|---|---|---|---|---|
| **Sel** A | Nucleotide | | TCT/TTT | ATT/ACT | |
| | Amino acid | | **S7F** | **I47T** | |
| **Sel** B | Nucleotide | AAC/AGC | | | |
| | Amino acid | **N102S** | | | |
| **Sel C** | Nucleotide | AAC/AGC | GGG/AGG | | ATG/GTG |
| | Amino acid | **N102S** | **G8R** | | **M108V** |

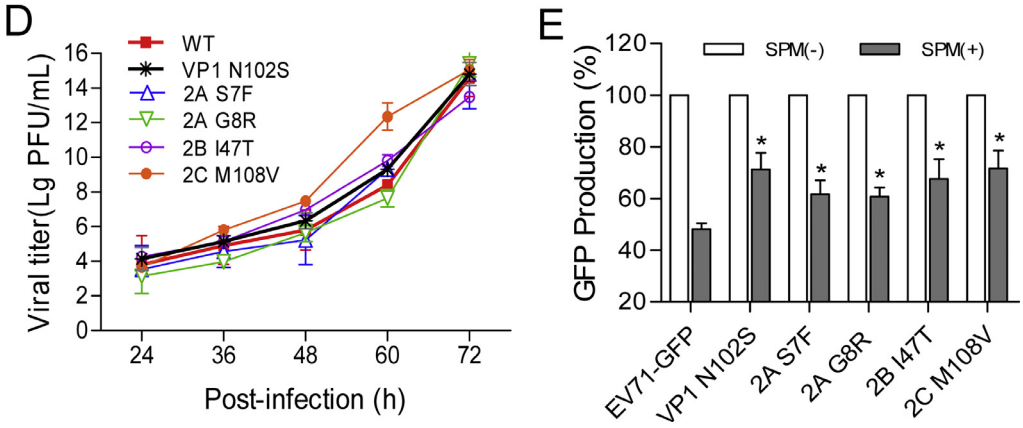


**Fig. 4.** Selection and determination of the mutations conferring resistance to spiramycin (SPM). (A) Selection scheme for SPM-resistant EV-A71. The concentrations of SPM along with the passage numbers are indicated. Three independent selections were performed. After 18 passages, the surviving viruses were collected, titrated and designated as SelA, SelB and SelC. (B) The susceptibility of these surviving viruses to SPM and azithromycin (AZM) was examined by viral titre reduction assay in Vero cells (multiplicity of infection (MOI), 0.1) in the presence of dimethyl sulphoxide (DMSO) alone, or with 50 μM of a drug. Forty-eight hours post-infection, the virus yields were measured. EV-A71 WT with indicated drugs was set as control in Student's *t* test analysis. * or #, $P<0.05$. (C) Sequence analysis of the surviving EV-A71 genome. The nucleotide mutations and the corresponding amino acid substitutions are indicated. (D) Growth kinetics of recombinant EV-A71-GFP variants. The recombinant EV-A71-GFP variants, each with one single mutation, were infected 293A-SCARB2 cells at an MOI of 0.001 PFU/cell. The viral yields at indicated different times post-infection were determined by plaque assay. The same procedure was performed with EV-A71-GFP wild type (WT) as a control. (E) Confirmation of the mutations conferring resistance to SPM through flow cytometry (FCM) assay. 293A-SCARB2 cells were infected with EV-A71-GFP WT or the recombinant variants at an MOI of 0.1 in the presence of DMSO (as a control) or 50 μM of SPM. At 24 h post-infection, GFP production was measured by FCM, with that of control cells set as 100%. All the results above are represented as mean ± standard deviation (SD) of three independent experiments. EV71-GFP treated with SPM was set as control in Student's *t* test analysis. *$P<0.05$.

These mutations were individually introduced into EV-A71-GFP and resulted in five recombinant EV-A71-GFP variants. Plague assay showed that the growth kinetics of these variants in 293A-SCARB2 cells were very similar to that of EV-A71-GFP WT, except that the variant with 2C-M108V mutation replicated faster than other viruses (Fig. 4D). 293A-SCARB2 cells were infected with these variants or EV-A71-GFP WT, followed by treatment with SPM or DMSO alone as a control for 24 h, and then subjected to FCM assay. As shown in Fig. 4E, upon SPM treatment, the GFP production was reduced by approximately 55% for EV-A71-GFP WT, but less for all the recombinant EV-A71-GFP variants, the reduction ranging from 28% to 40%. These results indicated that all these mutations contributed to the resistance to SPM.

### *3.4. AZM protects mice from EV-A71 infection more significantly than SPM*

The in vivo activities of SPM and AZM against EV-A71 infection were investigated in a mouse model. Five-day-old BALB/c mice were infected i.p. with the mouse-adapted strain EV-A71-MZ-MA1

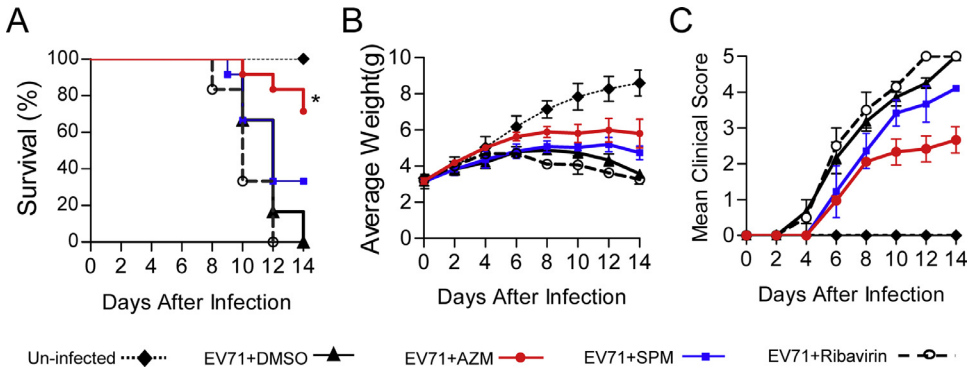


**Fig. 5.** Anti-infection efficacy of spiramycin (SPM) and azithromycin (AZM) in an EV-A71-infected mouse model. Five-day-old BALB/c mice were injected intraperitoneally (i.p.) with EV-A71-MZ-MA1 at a dose of $1 \times 10^7$ PFU each mouse. Subsequently, the mice were divided into four groups (six per group) and then given SPM, AZM, Ribavirin, or dimethyl sulphoxide (DMSO) alone i.p, once daily for 5 days, starting on the infection day. The mice without EV-A 71 infection were used as control. All the mice were monitored for survival (A), average weight (B) and clinical store (C) over the following 14 days. Scores were defined as: 0, healthy; 1, ruffled hair and hunchbacked appearance; 2, limb weakness; 3, paralysis in one limb; 4, paralysis in two limbs; 5, death. Data are expressed as mean ± standard deviation (SD) of three independent experiments. $^*P<0.05$.

and then given SPM or AZM i.p. once daily for five consecutive days, starting on the infection day. The administration doses of these two drugs were 30 mg/kg per day. Meanwhile, the antiviral agent ribavirin was given to the infected mice at the same dose as a control. The uninfected mice grew healthily; the infected mice given vehicle alone or ribavirin showed progressive severity in clinical symptoms and weight loss, followed by death 7–10 days post-infection; in contrast, SPM or AZM antagonized weight loss and improved the survival rate and clinical symptoms of the infected mice (Fig. 5A–C), suggesting an in vivo anti-EV-A71 activity. Noticeably, the survival rate of AZM-treated mice was 75%, twice as high as that of SPM-treated mice. Our additional mouse experiment showed that the anti-infection efficacy of AZM against EV-A71-MZ-MA1 was comparable to that of chloroquine (Supplementary Fig. S2), the latter which was reported to possess anti-EV-A71 activity in vivo [22]. Altogether, these results indicate that both SPM and AZM can protect mice from severe EV-A71 infection, and AZM has a stronger efficacy than SPM in vivo.

## 4. Discussion

In this work, we showed that SPM and AZM inhibited the replication of EV-A71 and CV-A16 in cell culture and improved the survival rate and disease manifestation in a mouse model of severe EV-A71 infection (Figs. 1C,D, 5). In contrast, the antiviral agent ribavirin administered at the recommended treatment dose (30 mg/kg, once daily) [23] did not exhibit protective effects in the EV71-infected mouse model (Fig. 5). These data suggest that SPM and AZM are potential drugs for EV-A71 infection therapy. Despite a weaker anti-EV-A71 activity in vitro compared to SPM, AZM should be given more attention in our opinion, not only because of its higher efficacy against EV-A71 infection in vivo, but also due to its advantages in pharmacokinetic and safety profiles compared to other macrolides [24]. In addition, AZM suspension suitable for children is commercially available. All these facts will benefit the rapid development of AZM into a therapeutic anti-EV-A71 agent. Ribavirin is a nucleoside analogue with broad-spectrum antiviral activities. Previous studies have shown that ribavirin could reduce EV-A71-induced cytopathic effects and viral yields in cell culture [25]. However, the mouse protection assay data from different labs are controversial. Li et al. [26] reported that ribavirin (100 mg/kg, once daily) increased the survival rate from 27% to 70% after 12- to 14-day-old institute of cancer research (ICR) mice were infected with $1 \times 10^5$ PFU of the EV-A71 strain M2; Zhang et al. [27] reported that ribavirin (80 mg/kg, once daily) did not protect the 1-day-old ICR mice infected with $2.5 \times 10^6$ PFU of EV-A71. This inconsistence can be attributed to the differences in virus inoculation dose, virus strains, mouse age, mouse strains, etc. Our evaluation on the potential antiviral agent chloroquine against EV71 infection also provided evidence for this presumption. A survival rate of 81.8% was observed for the mice infected with $1 \times 10^7$ PFU of EV-A71-MZ-MA1 after treatment with chloroquine (Supplementary Fig. S2), in contrast to 50% survival rate of the mice infected with $2 \times 10^7$ PFU of EV-A71 (strain 5865/sin/00009) [22]. Therefore, although AZM is a promising therapeutic candidate for EV-A71 infection, more animal experiments using different mouse and EV-A71 strains should be carried out to confirm the protective efficacy. Simultaneously, the administration dosage and delivery method should be optimized to achieve better therapeutic effects.

Our data suggest that SPM inhibits EV-A71 replication most likely through hampering viral RNA synthesis (Figs. 2, 3), though the potential effects on viral RNA stability and viral polyprotein processing could not be excluded. The SPM-resistant EV-A71 variants also display resistance to AZM (Fig. 4B), indicating a common mechanism against EV71 replication. However, this proposed mechanism could not explain why AZM exerts stronger anti-infection efficacy in vivo (Fig. 5) but weaker anti-EV-A71 activity in the cell culture than SPM (Fig. 1C,D). Multiple studies have shown that the effects of macrolide antibiotics against human rhinovirus (HRV) and some other viruses causing respiratory infections are partially due to the anti-inflammatory and immuno-modulatory activity of these drugs [12]. Noticeably, AZM can induce interferon (IFN) and interferon-stimulated gene (ISG) responses and reduce HRV replication more significantly than other macrolides [28]. Although EV-A71 suppresses the induction of IFN and the subsequent expression of ISGs [29], IFN treatment is effective against EV-A71 infection [30,31], and our experimental results indicate that some ISGs are capable of inhibiting EV-A71 replication (unpublished data). The question whether the immune responses induced by macrolides play a role in the anti-EV-A71 activities is worthy of investigation.

The mutations conferring resistance to SPM were identified to be VP1-N102S, 2A-S7F, 2A-G8R, 2B-I47T and 2C-M108V. BLAST search revealed that these amino acid residues are almost completely conserved in different EV-A71 genotypes and in different EV-A71 strains, especially VP1-N102 and 2B-I47, whose substitutions were found in one out of 12441 EV71 protein sequences submitted to the NCBI database. These highly conserved residues are therefore expected to be necessary for the function of the viral

proteins in EV-A71 propagation and virulence. It has been well recognized that VP1 and 2A are responsible for receptor interaction and polyprotein processing, respectively. Some other studies indicate that these two proteins are also involved in viral RNA replication [32,33]. Although a few functional residues have been identified, the roles of VP1-N102, 2A-S7 and G8 are not defined yet. 2B has been identified to be an ion channel protein [34] and 2C mainly functions as a nucleoside triphosphatase [35]. Some studies suggested that these two proteins are related to viral RNA replication through involvement in the formation or maintenance of the replication complex [36,37]. Nonetheless, little is known about the precise functions of 2B and 2C proteins as well as their residues 2B-I47 and 2C-M108. It would be interesting to investigate whether these residues contribute to viral virulence and immune evasion, because VP1, 2A, 2B and 2C have been shown to be involved in these processes [29,38]. These studies will help to uncover the mechanism of the macrolide antibiotics against EV-A71 and to better understand the biology of EV-A71.

In conclusion, the macrolide antibiotics AZM and SPM, safe for infants and young children, possess anti-EV-A71 infection efficacy in vitro and in vivo. AZM is a promising therapeutic candidate for anti-EV-A71 infection; however, more animal experiments are required to confirm and optimize its efficacy.

## Funding

This research was supported by the grants from Guangdong Innovative Research Team Program (2009010058), Medical Scientific Research Foundation of Guangdong Province (A2016467) and Meizhou Science and Technology Program to X.G.

## Competing Interests

None declared.

## Ethical Approval

All the animal experimentation was approved by Ethics Committee of Zhongshan School of Medicine on Laboratory (Guangzhou, China).

## Supplementary materials

Supplementary material associated with this article can be found, in the online version, at doi:10.1016/j.ijantimicag.2018.12.009.

## References

[1] Huang CC, Liu CC, Chang YC, Chen CY, Wang ST, Yeh TF. Neurologic complications in children with enterovirus 71 infection. N Engl J Med 1999;341:936–942.
[2] Repass GL, Palmer WC, Stancampiano FF. Hand, foot, and mouth disease: identifying and managing an acute viral syndrome. Clev Clin J Med 2014;81:537–43.
[3] Li L, He Y, Yang H, Zhu J, Xu X, Dong J, et al. Genetic characteristics of human enterovirus 71 and coxsackievirus A16 circulating from 1999 to 2004 in Shenzhen, People's Republic of China. J Clin Microbiol 2005;43:3835–9.
[4] Lin JY, Chen TC, Weng KF, Chang SC, Chen LL, Shih SR. Viral and host proteins involved in picornavirus life cycle. J Biomed Sci 2009;16:103–27.
[5] Lozano G, Martínez-Salas E. Structural insights into viral IRES-dependent translation mechanisms. Curr Opin Virol 2015;12:113–20.
[6] Tan CW, Lai JKF, I-Ching S, Chan YF. Recent developments in antiviral agents against enterovirus 71 infection. J Biomed Sci 2014;21:14–24.
[7] Menninger JR. Mechanism of inhibition of protein synthesis by macrolide and lincosamide antibiotics. J Basic Clin Physiol Pharmacol 1995;6:229–50.
[8] Buret AG. Immuno-modulation and anti-inflammatory benefits of antibiotics: the example of tilmicosin. Can J Vet Res 2010;74:1–10.
[9] Wales D, Woodhead M. The anti-inflammatory effects of macrolides. Thorax 1999;54(Suppl 2):S58–62.
[10] Kudoh S, Azuma A, Yamamoto M, Izumi T, Ando M. Improvement of survival in patients with diffuse panbronchiolitis treated with low-dose erythromycin. Am J Respir Crit Care Med 1998;157:1829–32.
[11] Koh YY, Lee MH, Sun YH, Sung KW, Chae JH. Effect of roxithromycin on airway responsiveness in children with bronchiectasis: a double-blind, placebo–controlled study. Eur Respir J 1997;10:994–9.
[12] Min JY, Yong JJ. Macrolide therapy in respiratory viral infections. Mediat Inflamm 2012;1:649570–9.
[13] Straypedersen B. Treatment of toxoplasmosis in the pregnant mother and newborn child. Scand J Infect Dis Suppl 1992;84:23–31.
[14] Wallon M, Gandilhon F, Peyron F, Mojon M. Toxoplasmosis in pregnancy. Lancet 1994;344:540–1.
[15] Zhang X, Pan Y, Nan W, Zhang J, Li J, Hao G, et al. The binding of a monoclonal antibody to the apical region of SCARB2 blocks EV71 infection. Protein Cell 2017;8:590–600.
[16] Li X, Liu Y, Wu T, Jin Y, Cheng J, Wan C, et al. The antiviral effect of baicalin on enterovirus 71 in vitro. Viruses 2015;7:4756–71.
[17] Zhou S, Chen X, Meng X, Zhang G, Wang J, Zhou D, et al. "Roar" of blaNDM-1 and "silence" of blaOXA-58 co-exist in Acinetobacter pittii. Sci Rep 2015;5:8976–7.
[18] Li K, Zhou S, Guo Q, Chen X, Lai DH, Lun ZR, et al. The eIF3 complex of Trypanosoma brucei: composition conservation does not imply the conservation of structural assembly and subunits function. RNA 2017;23:333–45.
[19] Deng C. Inhibition of enterovirus 71 by adenosine analog NITD008. J Virol 2014;88:11915–23.
[20] Shang B, Deng C, Ye H, Xu W, Yuan Z, Shi PY, et al. Development and characterization of a stable eGFP enterovirus 71 for antiviral screening. Antivir Res 2013;97:198–205.
[21] Patel DH, Seung GW, Hyeun JB. Modification of overlap extension PCR: a mutagenic approach. Indian J Biotechnol 2009;8:183–6.
[22] Tan YW, Wan KY, Sun J, Chu JJH. An evaluation of chloroquine as a broad-acting antiviral against Hand, Foot and Mouth Disease. Antivir Res 2017;149:143–9.
[23] World Health Organization. Application for inclusion of ribavirin in the WHO model list of essential medicines. The Expert Committee on the Selection and Use of Essential Medicines Policy, Access and Rational Use Swizerland; 2006.
[24] Jain R, Danziger LH. The macrolide antibiotics: a pharmacokinetic and pharmacodynamic overview. Curr Pharm Design 2004;10:3045–53.
[25] Zhang Y, Zhu Z, Zhu SL, An HQ, Yang ZH, Guo XB, et al. In vitro study on the effect of ribavirin reducing the EV71 replication. Chin J Exp Clin Virol 2009;23:44–6.
[26] Li ZH, Li CM, Ling P, Shen FH, Chen SH, Liu CC, et al. Ribavirin reduces mortality in enterovirus 71-infected mice by decreasing viral replication. J Infect Dis 2008;197:854–7.
[27] Zhang G, Zhou F, Gu B, Ding C, Feng D, Xie F, et al. In vitro and in vivo evaluation of ribavirin and pleconaril antiviral activity against enterovirus 71 infection. Arch Virol 2012;157:669–79.
[28] Porter JD. The innate anti-viral effects of Azithromycin and other novel macrolides. London, UK: PhD thesis Imperial College London; 2014.
[29] Pathinayake PS, Hsu AC, Wark PAB. Innate immunity and immune evasion by Enterovirus 71. Viruses 2015;7:6613–30.
[30] Liu ML, Lee YP, Wang YF, Lei HY, Liu CC, Wang SM, et al. Type I interferons protect mice against enterovirus 71 infection. J Genl Virol 2005;86:3263–9.
[31] Yi L, He Y, Chen Y, Kung HF, He ML. Potent inhibition of human enterovirus 71 replication by type I interferon subtypes. Antivir Ther 2011;16:51–8.
[32] Zhang YX, Huang YM, Li QJ, Li XY, Zhou YD, Guo F, et al. A highly conserved amino acid in VP1 regulates maturation of enterovirus 71. PLoS Pathog 2017;13:e1006625.
[33] Li C, Qiao Q, Hao SB, Dong Z, Zhao L, Ji J, et al. Nonstructural protein 2A modulates replication and virulence of Enterovirus 71. Virus Res 2017;244.
[34] Cong H, Du N, Yang Y, Song L, Zhang W, Tien P. Enterovirus 71 2B induces cell apoptosis by directly inducing the conformational activation of the proapoptotic protein Bax. Plos Pathog 2016;90:9862–77.
[35] Xia H, Wang P, Wang GC, Yang J, Sun X, Wu W, et al. Human enterovirus nonstructural protein 2C ATPase functions as both an RNA helicase and ATP-independent RNA chaperone. Plos Pathog 2015;11:e1005067.
[36] Johnson KL, Sarnow P. Three poliovirus 2B mutants exhibit noncomplementable defects in viral RNA amplification and display dosage-dependent dominance over wild-type poliovirus. J Virol 1991;65:4341–9.
[37] Barton DJ, Flanegan JB. Synchronous replication of poliovirus RNA: initiation of negative-strand RNA synthesis requires the guanidine-inhibited activity of protein 2C. J Virol 1997;71:8482–9.
[38] Liu Y, Fu C, Wu S, Chen X, Shi Y, Zhou B, et al. A novel finding for enterovirus virulence from the capsid protein VP1 of EV71 circulating in mainland China. Virus Genes 2014;48:260–72.